AIP Applied Physics Letters

Cost effective nanostructured copper substrates prepared with ultrafast laser pulses for explosives detection using surface enhanced Raman scattering

Syed Hamad, G. Krishna Podagatlapalli, Md. Ahamad Mohiddon, and Venugopal Rao Soma

Citation: Applied Physics Letters **104**, 263104 (2014); doi: 10.1063/1.4885763
View online: http://dx.doi.org/10.1063/1.4885763
View Table of Contents: http://scitation.aip.org/content/aip/journal/apl/104/26?ver=pdfcov
Published by the AIP Publishing

Cost effective nanostructured copper substrates prepared with ultrafast laser pulses for explosives detection using surface enhanced Raman scattering

Syed Hamad,[1] G. Krishna Podagatlapalli,[2] Md. Ahamad Mohiddon,[3] and Venugopal Rao Soma[2,a)]
[1]*School of Physics, University of Hyderabad, Prof. C. R. Rao Road, Hyderabad 500046, India*
[2]*Advanced Center of Research in High Energy Materials (ACRHEM), University of Hyderabad, Prof. C. R. Rao Road, Hyderabad 500046, India*
[3]*Center for Nanotechnology, University of Hyderabad, Prof. C. R. Rao Road, Hyderabad 500046, India*

(Received 12 February 2014; accepted 17 June 2014; published online 30 June 2014)

Ultrafast laser pulses induced surface nanostructures were fabricated on a copper (Cu) target through ablation in acetone, dichloromethane, acetonitrile, and chloroform. Surface morphological information accomplished from the field emission scanning electron microscopic data demonstrated the diversities of ablation mechanism in each case. Fabricated Cu substrates were utilized exultantly to investigate the surface plasmon (localized and propagating) mediated enhancements of different analytes using surface enhance Raman scattering (SERS) studies. Multiple utility of these substrates were efficiently demonstrated by collecting the SERS data of Rhodamine 6G molecule and two different secondary explosive molecules such as 5-amino-3-nitro-l,2,4-triazole and trinitrotoluene on different days which were weeks apart. We achieved significant enhancement factors of $>10^5$ through an easily adoptable cleaning procedure. © *2014 AIP Publishing LLC*. [http://dx.doi.org/10.1063/1.4885763]

Surface enhanced Raman spectroscopy (SERS)[1–8] is surface dependent spectroscopic technique, utilizing typically metal nano-structures, which allows enhancement of the Raman signal from adsorbed analyte species of very low concentration. SERS is one of the most capable techniques for detection of trace level explosive molecules[9,10] such as RDX (1,3,5-trinitroperhydro-1,3,5-triazine) and TNT (Trinitrotoluene). Till date, reported enhancement factors (EFs) in SERS experiments were in the range of $\sim 10^4$–10^8 with a few groups reporting higher ($>10^{12}$) factors in the case of single molecular detection. Electromagnetic mechanism[11–13] provokes the intensification of weak incident electromagnetic field by the excitation of surface plasmons which is a direct repercussion of plasmonic metal nanostructures (NSs) with high porosity. SERS intensity is proportional to the fourth power of electromagnetic field[14] which is related to complex dielectric function of metals. Ag and Au nanostructures have been extensively used as SERS active substrates[15–20] because they demonstrate largest signal enhancements compared to other metals since their optical properties are compatible to produce strong surface plasmon resonances in the visible/near-IR spectral range (400 nm–1000 nm). In contrast, copper NSs have been studied not as much as SERS active substrates because of thermal instability and partially compatible chemical properties. The main reason behind lower preference of Cu compared to Ag, particularly, is the intrinsic electronic configuration of the former which provides less ratio of real to imaginary parts of dielectric function (3.54–32.4). This ratio plays a crucial role in sustenance of plasmon resonances. Inherent oxidation effects of Cu metal demands extreme care for avoiding instantaneous oxidation prevailing at the time of fabrication of nanoparticles (NPs)/nanostructures.

Ultrafast laser ablation in aqueous media[21–24] is a pre-eminent method avoiding multistep chemical synthesis, long reaction times, and can overcome the demerit of Cu material with regard to oxidation. Laser ablation of metals in liquids provides an environment (oxygen free, polar, and poor capability to dissolve air) to minimize the effect of oxidation in the process of nanomaterials fabrication since ablation occurs underneath the liquid layer. Moreover, laser ablation of bulk metal target in suitable liquid media produce periodic (submicron dimensions) surface structures[23,25–29] for exploiting significant Raman enhancements via supporting the localized surface plasmon resonances (LSPRs) and Surface Plasmon Polaritons (SPPs). In addition to the specific liquid environments, multiple line/single line writing geometries can be utilized to enhance the probability of laser induced periodic surface structures (LIPSSs) formation. LIPSS align either parallel or perpendicular to input beam polarization and are expected due to the interference of incoming electric filed with surface electromagnetic waves (SEWs). These specially patterned surface structures assist in enhancing the Raman signatures even though the surface plasmons are weaker in Cu compared to silver or gold. Thus far, several groups have reported fabrication of periodic surface structures using ultrashort pulses for the case when laser fluences were beyond ablation threshold.[30,31] In this Letter, we present our results emphasizing the role of (a) different threshold fluences achieved through single and multiple exposures and (b) diverse organic solvent media resulting in different ablation products. In addition to LIPSS production, multiple utility of the patterned Cu targets is demonstrated. Moreover, the copper targets possess following advantages (a) they are more economic compared to Ag or Au targets (b) the cleaning procedures of laser ablated Ag/Ausubstrates[32–34] are cumbersome compared to Cu. It was observed that cleaning was a hard task in the case of plasmonic substrates which

[a)]Author to whom correspondence should be addressed. Electronic addresses: svrsp@uohyd.ernet.in and soma_venu@yahoo.com. Telephone: +91-040-23138811.

possessed long sustainable localized surface plasmons. For these substrates (especially Ag), a very difficult procedure is needed where as we demonstrate here that for Cu nanostructured surfaces nominal cleaning is sufficient to achieve superior performance (c) periodic patterning of copper is found to be favorable compared to more noble natured Ag or Au. In this Letter, we have investigated the (a) influence of multiple/single line ablation morphologies on eight Cu targets and the effect of surrounding medium, (b) SERS detection of explosive materials (ANTA, 5-amino-3-nitro-l,2,4-triazole) using Cu NSs fabricated via ultrafast multiple/single line ablation, and (c) Cu NSs substrates have been reused for 2 more times for SERS studies of other analytes such as TNT (2,4,6-trinitrotoluene) and rhodamine 6G (R6G).

Complete experimental details are presented in our earlier works.[23,25,28,29,35] The substrate was purchased locally, fixed in a glass cell and covered by transparent liquids [acetone, dichloromethane (DCM), acetonitrile (ACN), and chloroform]. Typical liquid level was ~7 mm above the surface. The cell was placed on X-Y motorized stages. The cell was scanned with speeds of ~0.1 mm/s in both the directions. The diameter ($2\omega_0$) of laser spot on target surface (in liquid) was estimated to be ~50 μm. Ablation was performed to draw periodic lines on surface to invoke (a) overwriting of the target surface for several times which is denoted as multiple line ablation [since the beam waist (~50 μm) was much higher than the scan separation (5 μm)] (b) single line ablation where line structures were drawn (without overlapping) with a given spacing of ~60 μm. The average number of pulses per spot on the target was ~4000 in the case of multiple line ablation and ~500 in the case of single line ablation (0.1 μm/ms speed and 1 pulse/ms incident on target). Characterization and applications of the generated Cu NPs were reported earlier.[35] To avoid ambiguity, Cu NSs prepared through multiple line (single line) ablation in acetone, DCM, ACN, and chloroform are labeled as MCuNS1 (SCuNS1), MCuNS2 (SCuNS2), MCuNS3 (SCuNS3), and MCuNS4 (SCuNS4), respectively.

Picosecond (~2 ps) laser machined Cu substrates were preserved after proper cleaning to remove any surface contaminations. Figure 1 illustrates the field emission scanning electron microscopic (FESEM-Ultra 55 from Carl ZEISS) images of fabricated NSs on the surface of Cu ablated in (a) acetone (MCuNS1), (b) DCM (MCuNS2), (c) ACN (MCuNS3), and (d) chloroform (MCuNS4) and insets present the images with a lower resolution (2 μm scale). Surface morphology of multiply ablated Cu substrates MCuNS1 [Figure 1(a)] and MCuNS3 [Figure 1(c)] revealed the formation of weakly distinguishable LIPSS with period of ~400 nm along with cylindrical Cu NPs grains (length ~ 300 nm and diameter ~ 20 nm) and the formation of LIPSS with a periodicity 250–300 nm, respectively. In the case of MCuNS2 [Figure 1(b)], surface topography of Cu substrate consisted of pillar shaped structures of few μm size. Moreover, most of the cubic NPs with size of ~200 nm were formed on the top of pillars. Similarly, in the case of MCuNS4 [Figure 1(d)], rough ended pillars with few μm sizes were formed on the surface. Figure 2 depicts the FESEM image morphologies of fabricated NSs on Cu substrates when ablation was carried out in (a) acetone

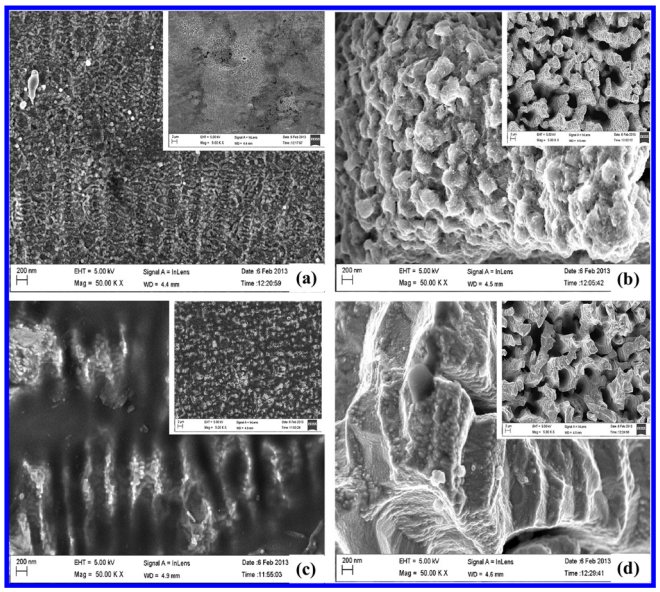

FIG. 1. FESEM images of substrates (a) MCuNS1 in acetone, (b) MCuNS2 in DCM, (c) MCuNS3 in ACN, and (d) MCuNS4 in $CHCl_3$ fabricated through ultrafast multiple line ablation of Cu. Insets show their corresponding views on a larger scale (2 μm scale).

(SCuNS1), (b) DCM (SCuNS2), (c) ACN (SCuNS3), and (d) chloroform (SCuNS4) via single line ablation and insets of Figure 2 depict the images with lower resolution (2 μm scale). We estimated that smaller number of pulses (500) per spot were incident on surface compared to multiple line ablation case (~4000). LIPSS with a periods of ~300 nm and ~400 nm for SCuNP1 [Figure 2(a))] and SCuNP3 [Figure 2(c)], respectively, were observed. In addition to this, spherical NP grains (with NP size of ~50 nm) were formed on the periodic structure surfaces in the case of SCuNP1, which was not observed in SCuNP3 case. Similarly, randomly corrugated structures along with NP grains and a small number of triangular NPs (~250 nm

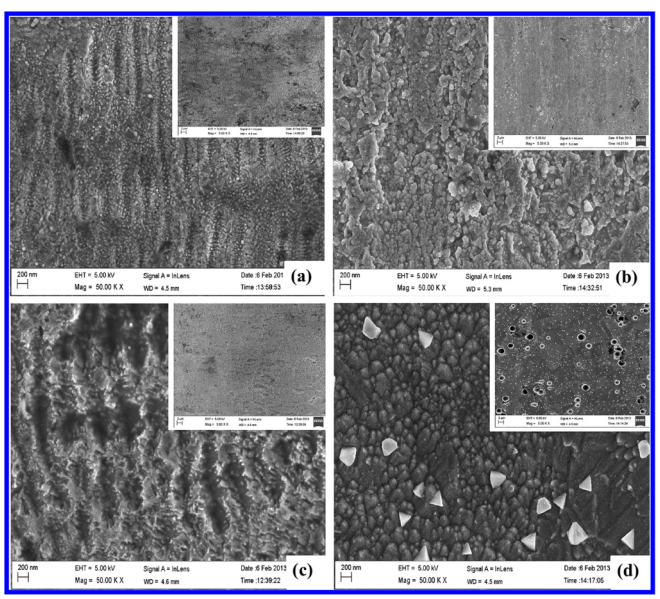

FIG. 2. FESEM images of substrates (a) SCuNS1 in acetone, (b) SCuNS2 in DCM, (c) SCuNS3 in ACN, and (d) SCuNS4 in chloroform fabricated through ultrafast single line ablation of Cu. Insets show corresponding views on a larger scale (2 μm scale).

size) were observed in the case of SCuNP2 [Figure 2(b)] and SCuNP4 [Figure 2(d)], respectively.

Earlier works on LIPSS have suggested that the observed ripples could be resultant of interference of the incident electromagnetic wave and surface scattered electromagnetic wave.[36] Furthermore, liquid media plays a dominant role in the formation of ripple structures which was evident from FESEM images. Since the properties of liquid medium interacting with the metallic plasma plume is different, redistribution of metallic melt under the influence of recoil pressure (which depends on latent heat of vaporization) of liquid molecules was different. Consequently, different nanostructures were obtained. The periodicity of the ripples is related to wavelength and angle of incidence as

$$\wedge_{\perp} = \frac{\lambda}{\frac{\lambda}{\lambda_S} \pm \sin\theta},$$

where $\wedge_{\perp}$ is the period of ripples, λ is the incident wavelength of the laser, λ_s is the wavelength of the surface waves, and θ is the angle of laser incidence (with normal) on target surface. For a normal incidence ($\theta = 0°$), periodicity of the ripples is almost equal to the wavelength of SEW.

Raman spectra of various analytes [ANTA (solvent-acetonitrile), TNT (solvent-acetonitrile), and R6G (solvent-methanol) of concentrations 10^{-4} M and 10^{-6} M] were recorded using a micro-Raman spectrometer (WITec-Alpha 300) with an excitation source of 532 nm wavelength and a 100X objective. Typically, a tiny drop ($\sim$10 μl) of ANTA was placed on all of the 8 Cu NS substrates to achieve a monolayer of the analyte molecules. Raman spectra were typically recorded for four times at various positions on the target and their average spectra were considered. Later on, utilized Cu substrates were cleaned and sonicated with acetonitrile and again the same substrates were utilized for the second time to record Raman spectra of R6G. Subsequently, proper cleaning procedures were again followed and the same substrates were once more utilized, for the third time, to record Raman spectra of TNT. The time separation between these three trials was approximately few weeks.

Raman spectra of ANTA from Cu NSs fabricated via ultrafast multiple and single line ablations are shown in Figures 3(a) and 3(b). Significantly, observed modes from the data were C-NO_2 symmetric stretching mode (1341 cm^{-1}),[37] N-N symmetric stretching mode (1130 cm^{-1}), NO_2 deformation + ring deformation (840 cm^{-1}), ring torsion + NO_2 deformation (589 cm^{-1}), C–N symmetric stretch mode (1480 cm^{-1}), N4-C5-N1 bending mode (960 cm^{-1}), ring deformation mode (1070 cm^{-1}), and ring def + N–H bend (1303 cm^{-1}). In the case of ANTA, large Raman signal enhancements were observed from MCuNS1 and SCuNS1. In particular, MCuNS1 (SCuNS1) nano-cylindrical grains (nanoparticle grains) were observed on the top of LIPSS. Consequently, these substrates could have provided high local fields which resulted in the observed strong enhancements. We also believe that for these surfaces effects of propagating and localized surface plasmons are probably appended. Raman spectra of ANTA from Cu substrates were compared with normal Raman spectra of ANTA obtained using Si target to estimate the EFs for 1341 cm^{-1} mode using the following formula:[38,39]

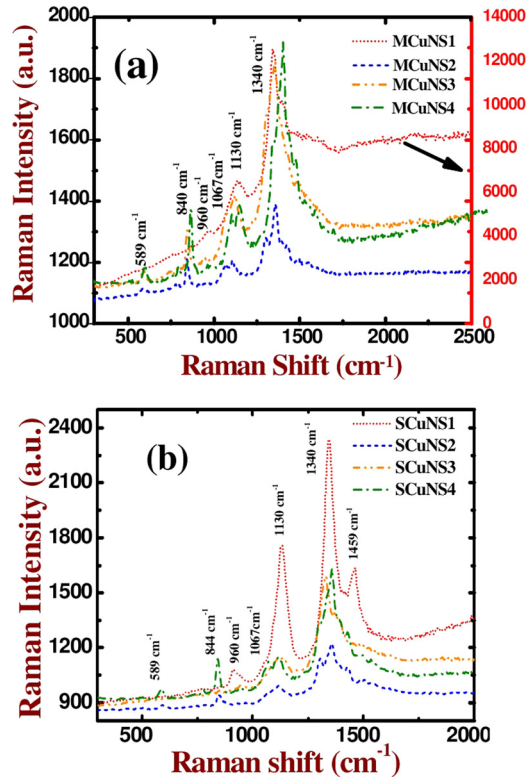

FIG. 3. SERS spectra recorded from ANTA molecule adsorbed on different (a) multiple line and (b) single line ablated Cu NSs. MCuNS1 (SCuNS1)-red/short dotted line, MCuNS2 (SCuNS2)-blue/short dashed line, MCuNS3 (SCuNS3)-orange/dash-dot-dot line, and MCuNS4 (SCuNS4)-olive/dash dot line. The integration time was 5 s.

$$E.F = \frac{I_{SERS}}{I_{Raman}} \frac{N_{Raman}}{N_{SERS}}, \quad (1)$$

where I_{SERS} is the intensity of surface enhanced signal (at lower concentration), N_{SERS} is the number of molecules participating in the enhancement of Raman signal (at lower concentration), I_{Raman} is the intensity of normal Raman signal of analyte (at higher concentration) collected from a plain silicon surface (see supplementary material), and N_{Raman} is the number of molecules contributing to the normal Raman signal of analyte at higher concentration. The intensity for 1341 cm^{-1} mode for MCuNP1 was $\sim$5301 (arbitrary units). However, the normal Raman intensity of ANTA from Si target for the same mode recorded with similar experimental conditions was $\sim$10 (arbitrary units). The intensity enhancement (I_{SERS}/I_R), therefore, was estimated to be $\sim$530. We estimated that $\sim$50% of analyte molecules were adsorbed on the Cu substrates [the adsorption coefficient (η) used was $\sim$0.5. Details of adsorption coefficient estimation are provided in supplementary material[40]]. EFs calculated for the 1340 cm^{-1} mode of ANTA molecule were 1.2×10^6, 3.1×10^4, 7.3×10^4, 7.1×10^4, 1.4×10^5, 3.6×10^4, 7.1×10^4, and 7×10^4 for MCuNS1, MCuNS2, MCuNS3, MCuNS4, SCuNS1, SCuNS2, SCuNS3, and SCuNS4, respectively.[40]

Similarly, Raman spectra of R6G (data presented in Figure 4) from the cleaned multiply and singly ablated Cu substrates recorded for the second time were analyzed. The prominent enhanced modes of R6G were the aromatic C-C stretch, C-H out plane bend, and C-C-C ring in plane bend at1363 cm^{-1}, 772 cm^{-1}, and 610 cm^{-1}, respectively. Evaluation of EFs was

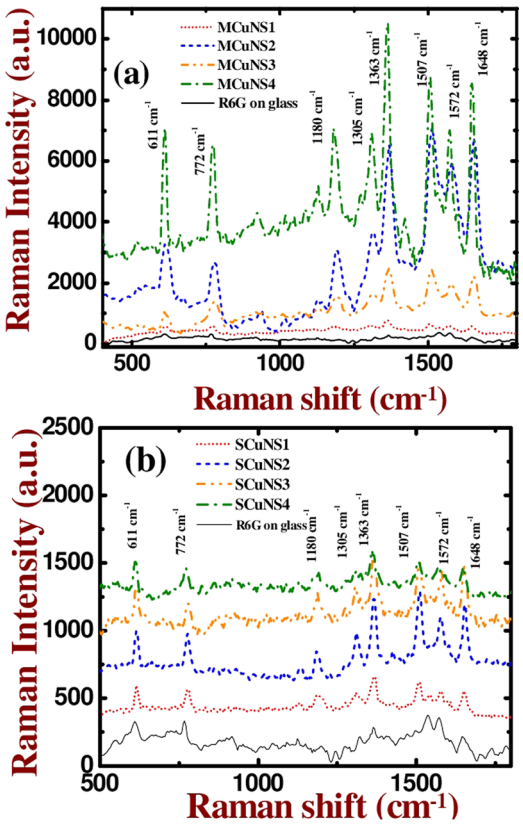

FIG. 4. SERS spectra recorded from R6G molecule adsorbed on different (a) multiple line and (b) single line ablated Cu NSs. MCuNS1 (SCuNS1)-red/short dotted line, MCuNS2 (SCuNS2)-blue/short dashed line, MCuNS3 (SCuNS3)-orange/dash dot dotted line, MCuNS4 (SCuNS4)-olive/dash dotted line, and R6G on glass-black solid lines. The integration time was 5 s.

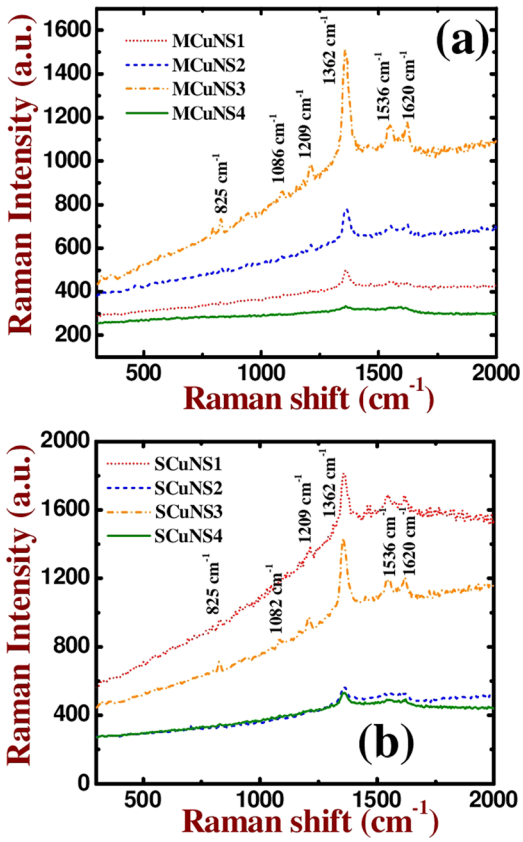

FIG. 5. SERS spectra recorded from TNT molecule adsorbed on different (a) multiple line and (b) single line ablated Cu NSs. MCuNS1 (SCuNS1)-red/short dotted line, MCuNS2 (SCuNS2)-blue/short dashed line, MCuNS3 (SCuNS3)-orange/short dash dotted line, and MCuNS4 (SCuNS4)-olive/solid line. The integration time was 5 s.

carried out by comparing reference spectra of R6G (0.25M concentration) recorded from a cover slip. At low concentrations ($\sim$5 μM) of R6G, it is believed from the adsorption factor calculations (see supplementary material) that 43% of molecules ($\eta \sim 0.43$) are adsorbed on Cu NS substrates. Estimated EFs of R6G for the1363 cm^{-1} mode were 6.2×10^5, 9.1×10^6, 2.6×10^6, 1.8×10^7, 4.6×10^5, 1.1×10^6, 9.1×10^5, and 3.8×10^5 for MCuNS1, MCuNS2, MCuNS3, MCuNS4, SCuNS1, SCuNS2, SCuNS3, and SCuNS4, respectively.[40] Among the substrates investigated MCuNS2, whose surface topography comprised of micron sized pillars, and MCuNS4, containing roughened pillars along with nanoparticle grains, demonstrated stronger enhancements.[23]

Raman spectra of the third testing sample TNT were recorded from the 8 Cu targets subsequent to proper cleaning and are illustrated in Figure 5. The recorded Raman spectra revealed that NO_2 symmetrical stretch[9] mode corresponding to 1362 $cm^{-1}$was predominantly elevated. Additionally, two more peaks were observed, one at 1616 cm^{-1} which corresponds to C-C aromatic stretching vibration and another mode at 790 cm^{-1} (C-H out of plane bend). Corresponding EF's calculated for 1362 cm^{-1} mode were $\sim 4.2 \times 10^4$, $\sim 7.7 \times 10^4$, $\sim 2.2 \times 10^5$, $\sim 1.6 \times 10^4$, $\sim 2.5 \times 10^5$, $\sim 5.8 \times 10^4$, $\sim 1.9 \times 10^5$, and $\sim 5.2 \times 10^4$ for MCuNS1, MCuNS2, MCuNS3, MCuNS4, SCuNS1, SCuNS2, SCuNS3, and SCuNS4, respectively.

Raman spectra collected from three analytes using the same Cu targets demonstrated a small reduction in enhancements from analyte 1 to analyte 3. However, the enhancements were reasonably large even in the third trial. Our experimental data demonstrated that nanostructured Cu targets possess potential for elevating the Raman signatures of diverse analytes. We believe that there could be two possible reasons behind the Raman signal enhancement. First reason is the coupling of incident photons to localized surface plasmons leading to the elevation of evanescent fields.[8] These evanescent fields influences the individual vibrating dipoles to re-radiate large number of photons thus enhancing the Raman signal. The mentioned coupling of incident photons to LSP should satisfy the condition that dimensions and shape of the nanomaterial[8] must execute perpendicular surface plasmon vibrations with respect to surface of the target. Second, whenever the separation between the nano-dimensional materials (nanoparticles or nano-tips) is optimal then the combined electron resonances of individual structures enhance the probability of coupling and hence enormous amount of evanescent fields[41] are possible sometimes specifically compatible with certain modes of interest. Aforesaid dynamics boost up the enhancements to substantially significant amount. Consequently, some substrates demonstrated better Raman signature enhancement for a specific molecule. Estimated EFs in our experiments were significantly stronger compared to EFs obtained with Cu targets prepared by other methods.[42,43] Moreover, we believe that Cu is well suited for fabricating SERS active substrates via laser ablation at minimal costs compared to other plasmonic metals.[44]

We are also attempting to combine both nanostructures and nanoparticles for further enhancement in the Raman

signal. Our independent studies (performed separately) on copper colloids do indicate strong SERS signal. We intend to place these nanoparticles on nanostructures and repeat the SERS measurements. This kind of hybrid SERS techniques wherein we can use these substrates along with nanoparticles (both of them can be washed to obtain clean substrates again) will be a potential technique and could meet the detection limits for field deployment. Furthermore, following our recent NS's fabrication on Silicon targets[45] we could use them in two ways: (i) place plasmonic metal nanoparticles and analytes in these groves for SERS studies and (ii) since these structures are periodic one can coat Ag, Au, and Cu (simple evaporation or RF sputtering) layers and use them for SERS studies. These studies will be taken up in near future.

In summary, laser induced surface nanostructures were fabricated with periodicity less than 400 nm via single/multiple line ablation of Cu targets in various organic solvents using ultrafast ($\sim$2 ps) laser pulses. LIPSS were achieved through the selection of suitable liquid environment in which ablation was carried out. The reproducibility of the Cu targets for trace level detection of explosive molecules was dealt with a simple cleaning procedure. Trace level detection of explosive compounds such as ANTA and TNT was performed along with R6G individually after subjecting surfaces to appropriate cleaning procedures and obtained enhancement factors of $>10^5$.

S.H. acknowledges CSIR for SRF. V.R.S. acknowledges DRDO for financial assistance and CNF, UoH for Raman facility.

[1]K. Kneipp, Y. Wang, H. Kneipp, L. T. Perelman, I. Itzkan, R. R. Dasari, and M. S. Feld, Phys. Rev. Lett. **78**, 1667 (1997).
[2]M. Sun, Z. Zhang, L. Chen, and H. Xu, Adv. Opt. Mater. **1**, 449–455 (2013).
[3]A. K. Kalkana and S. J. Fonash, Appl. Phys. Lett. **89**, 233103 (2006).
[4]*Surface-Enhanced Raman Scattering-Physics and Applications*, edited by K. Kneipp M. Moskovits, and H. Kneipp (Springer, 2006).
[5]D. Natelson, Y. J. Li, and J. B. Herzog, Phys. Chem. Chem. Phys. **15**, 5262–5275 (2013).
[6]C. Wang, Y. C. Chang, J. Yao, C. Luo, S. Yin, P. Ruffin, C. Brantley, and E. Edwards, Appl. Phys. Lett. **100**, 023107 (2012).
[7]M. Muniz-Miranda, C. Gellini, and E. Giorgetti, J. Phys. Chem. C **115**, 5021 (2011).
[8]K. M. Kosuda, J. M. Bingham, K. L. Wustholz, and R. P. Van Duyne, Compr. Nanosci. Technol. **3**, 263 (2011).
[9]P. M. Fierro-Mercado and S. P. Hernandez-Rivera, Int. J. Spectrosc. **2012**, 716527.
[10]T. Ivan and H. Jörg, J. Raman Spectrosc. **44**, 536 (2013).
[11]M. Moscovits, J. Chem. Phys. **69**, 4159 (1978).
[12]J. I. Gersten and A. Nitzan, J. Chem. Phys. **73**, 3023 (1980).
[13]C. K. Chen, A. R. B. de Castro, and Y. R. Shen, Phys. Rev. Lett. **46**, 145 (1981).
[14]J. Fontana, J. Livenere, F. J. Bezares, J. D. Caldwell, R. Rendell, and B. R. Ratna, Appl. Phys. Lett. **102**, 201606 (2013).
[15]D. M. Kuncicky, S. D. Christesen, and O. D. Velev, Appl. Spectrosc. **59**, 401 (2005).
[16]M. Ahmad Mohiddon, S. L. D. Varma, and M. Ghanashyam Krishna, Chem. Phys. Lett. **588**, 160 (2013).
[17]K. Fukami, M. L. Chourou, R. Miyagawa, Á. M. Noval, T. Sakka, M. Manso-Silván, R. J. Martín-Palma, and Y. H. Ogata, Materials **4**, 791 (2011).
[18]Z. Dai, X. Xiao, L. Liao, J. Zheng, F. Mei, W. Wu, J. Ying, F. Ren, and C. Jiang, Appl. Phys. Lett. **103**, 041903 (2013).
[19]S. J. Henley, J. D. Carey, and S. R. P. Silva, Appl. Phys. Lett. **88**, 081904 (2006).
[20]S. Y. Han, Q. H. Guo, M. M. Xu, Y. X. Yuan, L. M. Shen, J. L. Yao, W. Liu, and R. A. Gu, J. Colloid Interface Sci. **378**, 51 (2012).
[21]T. Y. Hwang, A. Y. Vorobyev, and C. Guo, Appl. Phys. Lett. **95**, 123111 (2009).
[22]I. Lee, S. W. Han, and K. Kim, J. Raman Spectrosc. **32**, 947 (2001).
[23]G. K. Podagatlapalli, S. Hamad, S. P. Tewari, S. Sreedhar, M. D. Prasad, and S. Venugopal Rao, J. Appl. Phys. **113**, 073106 (2013).
[24]A. Chou, E. Jaatinen, R. Buividas, G. Seniutinas, S. Juodkazis, E. L. Izake, and P. M. Fredericks, Nanoscale **4**, 7419 (2012).
[25]G. K. Podagatlapalli, S. Hamad, S. Sreedhar, S. P. Tewari, and S. Venugopal Rao, Chem. Phys. Lett. **530**, 93 (2012).
[26]Y. Yang, J. Yang, C. Liang, H. Wang, X. Zhu, and N. Zhang, Opt. Express **17**, 21124 (2009).
[27]G. Miyaji and K. Miyazaki, Opt. Express **16**, 16265 (2008).
[28]G. K. Podagatlapalli, S. Hamad, and S. Venugopal Rao, Appl. Surf. Sci. **303**, 217 (2014).
[29]S. Venugopal Rao, G. K. Podagatlapalli, and S. Hamad, J. Nanosci. Nanotechnol. **14**, 1364 (2014).
[30]J. Wang and C. Guo, Appl. Phys. Lett. **87**, 251914 (2005).
[31]J. W. Yao, C. Y. Zhang, H. Y. Liu, Q. F. Dai, L. J. Wu, S. Lan, A. Venu Gopal, V. A. Trofimov, and M. L. Tatiana, Opt. Express **20**, 905 (2012).
[32]Q. Su, X. Ma, J. Dong, C. Jiang, and W. Qian, ACS Appl. Mater. Interfaces **3**, 1873 (2011).
[33]Y. Wang, N. Lu, W. Wang, L. Liu, L. Feng, Z. Zeng, H. Li, W. Xu, Z. Wu, W. Hu, L. Lu, and L. Chi, Nano Res. **6**, 159 (2013).
[34]L. Yang, Z. Bao, Y. Wu, and J. Liu, J. Raman Spectrosc. **43**, 848 (2012).
[35]S. Hamad, G. K. Podagatlapalli, S. P. Tewari, and S. Venugopal Rao, J. Phys. D: Appl. Phys. **46**, 485501 (2013).
[36]U. Chakravarty, R. A. Ganeev, P. A. Naik, J. A. Chakera, M. Babu, and P. D. Gupta, J. Appl. Phys. **109**, 084347 (2011).
[37]J. A. Ciezak and S. F. Trevino, Chem. Phys. Lett. **403**, 329 (2005).
[38]E. C. Le Ru, E. Blackie, M. Meyer, and P. G. Etchegoin, J. Phys. Chem. C **111**, 13794 (2007).
[39]Y. Yang, Z. Y. Li, K. Yamaguchi, M. Tanemura, Z. R. Huang, D. L. Jiang, Y. H. Chen, F. Zhou, and M. Nogami, Nanoscale **4**, 2663 (2012).
[40]See supplementary material at http://dx.doi.org/10.1063/1.4885763 for complete details of adsorption factor and EF calculations.
[41]L. Gunnarsson, E. J. Bjerneld, H. Xu, S. Petronis, B. Kasemo, and M. Käll, Appl. Phys. Lett. **78**, 802 (2001).
[42]B. Lu-Yang Chen, J. Yu, T. Fujita, and M. Chen, Adv. Funct. Mater. **19**, 1221 (2009).
[43]J. Cejkova, V. Prokopec, S. Brazdova, A. Kokaislova, P. Matejka, and F. Stepanek, Appl. Surf. Sci. **255**, 7864 (2009).
[44]L. Polavarapu and L. M. Liz-Marzán, Phys. Chem. Chem. Phys. **15**, 5288 (2013).
[45]S. Hamad, G. K. Podagatlapalli, V. S. Vendamani, S. V. S. Nageswara Rao, A. P. Pathak, S. P. Tewari, and S. Venugopal Rao, J. Phys. Chem. C **118**, 7139 (2014).